Simulations and cold-test results of a prototype plane wave transformer linac structure

Arvind Kumar, K. K. Pant, and S. Krishnagopal

Beam Physics & FEL Laboratory, Centre for Advanced Technology, Indore-452013, India

We have built a 4-cell prototype plane wave transformer (PWT) linac structure. We discuss here details of the design and fabrication of the PWT linac structure. We present results from SUPERFISH and GDFIDL simulations as well as cold tests, which are in good agreement with each other. We also present detailed tolerance maps for the PWT structure. We discuss beam dynamics simulation studies performed using PARMELA.

I. INTRODUCTION

We are developing a high-brightness electron beam source for free-electron laser (FEL) applications, which incorporates an *S*-band photocathode rf gun [1] and a novel rf accelerating structure called the plane wave transformer (PWT) [2]. For moderate energies, the PWT linac structure has proven to compare favorably with conventional linac structures in terms of electrical properties such as shunt impedance, quality factor, etc. [3,4]. Besides this, it is also simple to evacuate due to its openness and easy to excite due to high intercell coupling. An additional advantage of the PWT structure is its ease of fabrication because of its relaxed dimensional tolerance due to the high intercell coupling of the electromagnetic fields. This was an important consideration in our choice to build a PWT structure.

The PWT linac was first proposed by Andreev in the 1960s [5] as a linear proton accelerator, but the first accelerating structure of its kind was fabricated by Swenson in 1988 [3], which was followed by the research group at UCLA with many improvements in the original structure [6]. The UCLA group built the first, and to date only, operating PWT linac, which is presently being used for free-electron laser applications. The PWT linac structure we are building is similar to the PWT3 structure at UCLA and is proposed to be used to drive a far-infrared FEL at 80 μm using a 10 MeV beam.

In this paper, we present detailed rf simulations performed using electromagnetic field solver codes SUPERFISH [7] and GDFIDL [8]. SUPERFISH calculates radio-frequency electromagnetic fields for axially symmetric cylindrical structures. This program generates a triangular mesh fitted to the boundaries of different material in the problem geometry. The direct sparse matrix method is used to evaluate the fields at each mesh point inside the structure. In spite of being a two-dimensional field solver code, SUPERFISH is very useful in fixing the preliminary dimensions of the accelerating structure. The particle dynamics simulations performed using PARMELA [9] also require field data generated by SUPERFISH; hence, SUPERFISH

simulations are essential for the beam dynamics study of the structure. GDFIDL, on the other hand, is a three-dimensional electromagnetic field solver code, which is used to simulate the asymmetric features (supporting/ cooling tubes) of the PWT linac structure. As expected, the results show a huge perturbation to the resonant frequency of the linac structure due to the presence of the tubes.

As the first step towards building the full 10 MeV PWT structure, we performed detailed simulations of the structure using the 2D code SUPERFISH to obtain a tolerance map of the resonant frequency of the structure to imperfections in its various dimensions. Some interesting results obtained from these simulations are discussed in the following sections, along with results obtained from 3D simulations performed later. Based on results obtained from 2D simulations, a 210.0 mm long, 4-cell (3 full + 2 half) prototype PWT1 structure was fabricated. A schematic of the fabricated structure is shown in Fig. 1. Simultaneously 3D simulations using GDFIDL were started with the first step being a comparison of results obtained using this code for a PWT1 linac without support tubes, with those obtained earlier using SUPERFISH. After this benchmarking of the 3D code, effects of the asymmetric elements in the designed PWT1 structure were studied, and subsequently compared with the results obtained from cold tests on the fabricated structure. Dummy PWT structures with disks of different diameters were also simulated and fabricated to have a better appreciation of the agreement between the resonant frequency predicted by GDFIDL, with those obtained from cold tests of the structure. In some cases, an agreement of about 1 MHz in about 2900 MHz was obtained, which is quite good.

Encouraged by these results, we built two more 4-cell prototypes, which were used both to solve various mechanical engineering issues in the fabrication and brazing of the structures, as well as to enlarge our database on the agreement between results obtained from simulations of the structure with those obtained from cold tests. With these issues sorted out, we have now successfully built and cold tested a 4-cell structure PWT3, which resonates
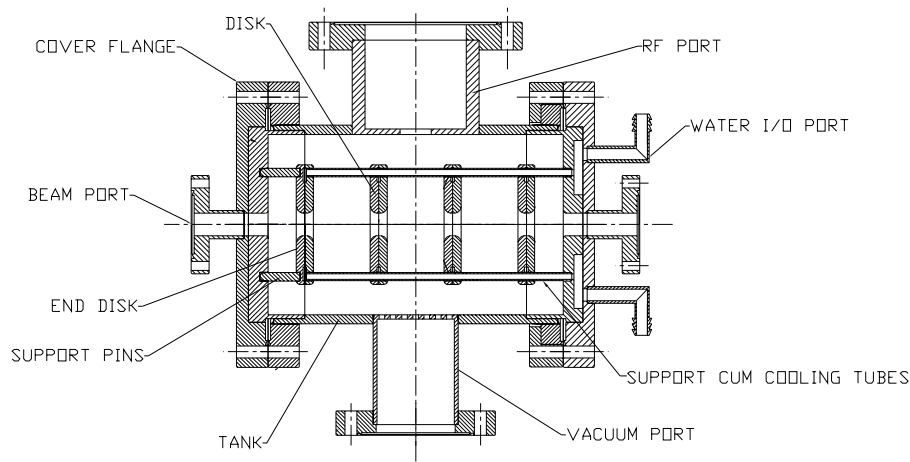
FIG. 1.   Schematic of the prototype, 4-cell, PWT linac structure.

at the design frequency of 2856 MHz, with a quality factor Q_L of around 10 000.

In the next section, we discuss results obtained from simulations of the structure using field solver codes SU-PERFISH and GDFIDL, based on the first prototype that was designed. In Secs. III–V, we present results obtained from cold tests of the prototype structures. We discuss particle dynamics simulations performed by using PARMELA in Sec. VI, followed by a summary of the results with conclusions and our plans for the future in Sec. VII.

II. SIMULATIONS

Our study of the first prototype PWT structure, PWT1, started with SUPERFISH simulations of the structure using the dimensions of the structure that were fixed to resonate at 2856 MHz in the π mode. Although SUPERFISH is a two-dimensional code and cannot simulate nonaxisymmetric components such as the support tubes, the results are useful for the first study of the structure to understand its electrical properties. Also, SUPERFISH gives the electric field distribution at every point inside the structure, which is used to fix the location of the support tubes in the region of the minimum electric field so as to cause a minimum perturbation in the resonant frequency of the structure. For the first prototype structure with disks of diameter 85.2 mm, support tubes were fixed at a radius of 36 mm. It should be noted that this is a zeroth order approximation since the tubes were expected to perturb the resonant frequency quite significantly. However, at that time we did not have access to a three-dimensional code.

A. Tubes

The actual placement of the tubes perturbs the electric field profile locally and could still perturb the resonant frequency quite significantly. However, at that time we did not have a three-dimensional rf code to simulate the actual structure. We therefore decided to go ahead with these

parameters, since our focus was on first mastering the mechanical engineering issues in the fabrication of the structure. Later we obtained the three-dimensional code GDFIDL, with which we simulated the actual structure, including the tubes, and found the resonance frequency to be 2969 MHz.

The actual position of the tubes strongly affects the resonant frequency. Figure 2 shows the variation of the resonant frequency of the structure with the location of the support tubes for fixed tubes and disks diameter. According to this, the tubes should be located in the flattest region of the curve which happens to be different from that predicted by SUPERFISH for disks of the same size. Since GDFIDL does a three-dimensional simulation of the structure, it is useful to determine the perturbations caused by non-axisymmetric elements inside the structure. The support tubes are found to increase the resonant frequency of the first prototype PWT structure, PWT1, by about 113 MHz in comparison to SUPERFISH results. GDFIDL also predicts a nonlinear dependence of the resonant frequency on the radial position of the support tubes on the disk (Fig. 2).
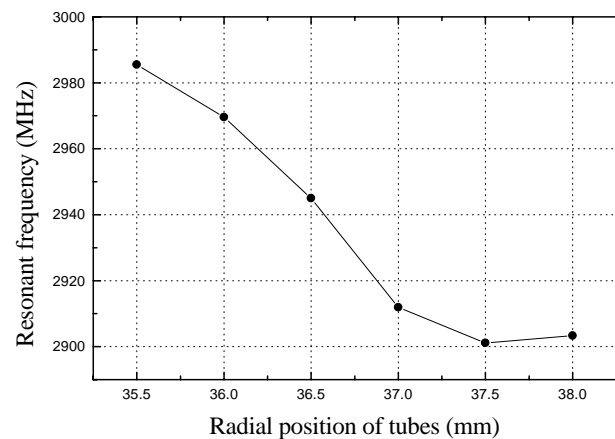
FIG. 2.   Variation of resonant frequency as a function of the location of the support/cooling tubes in the PWT structure.
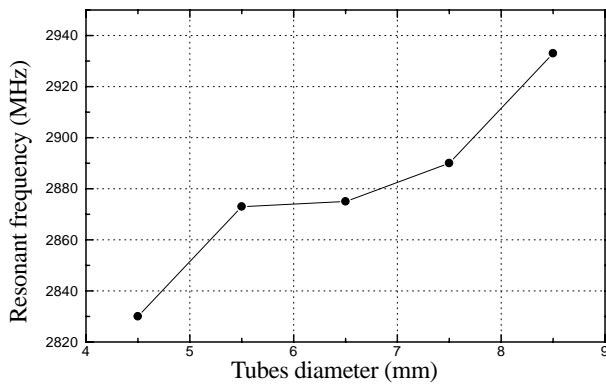
FIG. 3. Resonant frequency perturbation with supporting/ cooling tube diameter.

The diameter of the support tubes also perturbs the resonant frequency of the structure, even if the support tubes are inserted in the flat region of Fig. 2. We used GDFIDL simulations to study this effect, and found that the perturbation in the resonant frequency of the structure due to the tube diameter becomes very small at a diameter of 5.5 to 6.5 mm. These simulations are very important from the point of view of deciding the tubes diameter and errors in fabrication of the supporting tubes. An increase in the tubes diameter, for a fixed tubes pitch circle diameter (PCD) [10], increases the resonant frequency of the structure as shown in Fig. 3.

It should be noted here that the resonant frequency perturbation of the tubes diameter is not linear. Hence, 3D calculations using codes such as GDFIDL and MAFIA for the prediction of the tube diameter and its location on the disk are necessary.

B. Disks

The resonant frequency of the PWT structure is very sensitive to the disk outer diameter (OD), and both the codes SUPERFISH and GDFIDL were used for this study. GDFIDL simulations include the asymmetric features of the structure. Figure 4 shows resonant frequency perturbation due
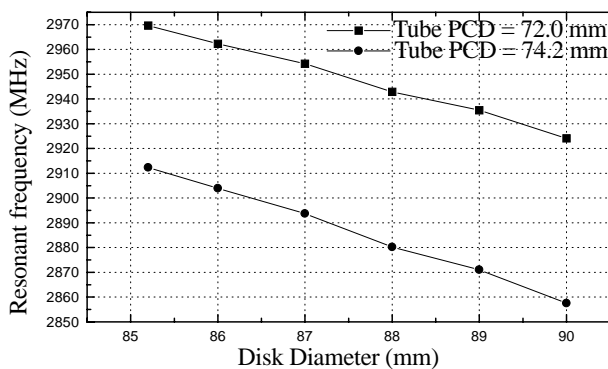
to the disks outer diameter keeping the tubes PCD fixed at one location. It is interesting to note that in 3D simulations, which consider the asymmetries of the PWT structure, the tubes initially located at a region of minimum electric field for a given disk outer diameter can come into a region of high electric field, as the disk OD is increased, but with the PCD kept the same as before. Thus, the combined effect of tubes with disks OD causes a lowering of the sensitivity of the resonant frequency on disk OD calculated by GDFIDL (10 MHz/mm) as compared to that obtained from SUPER-FISH (18 MHz/mm), where the tubes cannot be included in the calculation of resonant frequency [11].

C. Structure length

An interesting feature observed in the simulations is that the resonant frequency is more sensitive to any perturbation that causes an increase in the total length of the structure. If an increase in the length of one cell of the structure is compensated by a corresponding reduction in the length of the neighboring cells, it does not affect the resonant frequency significantly. This shows that in the PWT structure, there is no need to tune each cell. If, however, the increase in one cell length affects the total length of the structure, the resonant frequency varies by about 4 MHz/mm (Fig. 5). Although, there is no provision for tuning the PWT structure, fine-tuning can be achieved by the adjustment of the length of the end cells.

D. Others

SUPERFISH simulations are also useful in fixing the location of the cooling channel machined inside the disks. From the distribution of power dissipation on the surface of the disks, the location of the water channel is chosen to match the region of maximum power dissipation on the disk surface. To evolve a mechanical engineering drawing of the structure, extensive simulations were done to generate a tolerance map of the resonant frequency of the structure to machining errors, by physically introducing inaccuracies in different dimensions of the structure. This

FIG. 4. Effect of the the disks outer diameter on the resonant frequency of the PWT linac structure.
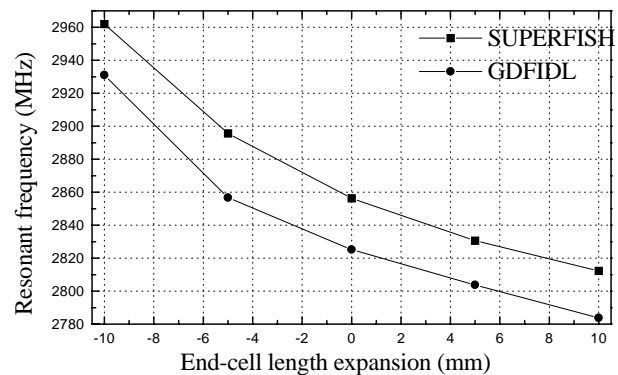
FIG. 5. Structure length effect on resonant frequency of the PWT linac structure.

helped us in fixing the geometric and dimensional tolerances for the machining of components of the structure based on which components of the first prototype PWT structure, PWT1, were fabricated [12].

E. PWT1 simulations

For the prototype PWT1 structure, the resonant frequency of the operating mode was expected to be different from that simulated by SUPERFISH because of the presence of the support/cooling tubes. This was confirmed using GDFIDL simulations, which predict a resonant frequency of 2969 MHz for the same structure in the presence of support/cooling tubes. Table I gives a comparison of the resonant frequency and electrical parameters of the first prototype PWT1 structure as predicted by SUPERFISH and GDFIDL simulations. Since the results differ significantly, extensive simulations were performed using GDFIDL to confirm the tolerance map obtained from SUPERFISH simulations [11].

GDFIDL simulations were also used to study the effect of rf and vacuum port openings on the resonant frequency of the structure. Since the vacuum port is a grid of small openings which do not affect the electrical continuity of the structure significantly, the resonant frequency is not affected much. The rf port opening, however, causes a perturbation of a few MHz in the resonant frequency of the PWT1 structure.

Figure 6 shows the dispersion curve of the modes supported by the structure as calculated by GDFIDL. For the TM_{01n} mode, the magnetic field profile shows a circulation around the tubes indicating a flow of current through them. Hence, operation in this mode is avoided to eliminate the large power dissipation that would occur on the tubes. The field profile for the TM_{02n} mode shows no such feature, and consequently PWT linac structures are normally operated in this higher order mode. This affects the frequency separation between neighboring modes, and consequently PWT linac structures cannot be made very long.

For the first prototype structure, the nearest neighboring mode for the operating π mode is the $3\pi/4$ mode with a separation of about 225 MHz. The bandwidth of the structure $f_\pi - f_0$ is 365 MHz giving an intercell coupling coefficient of 0.15.
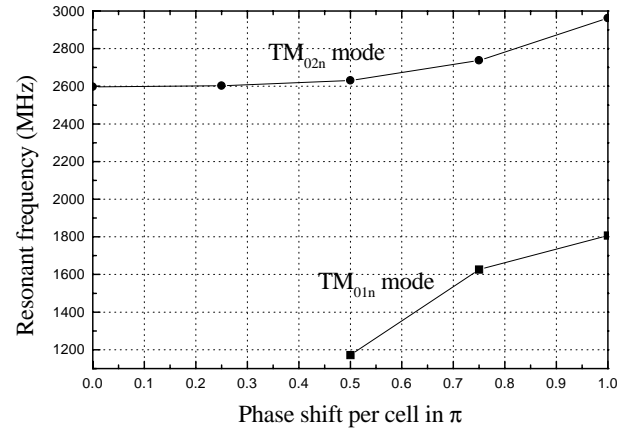
FIG. 6.   Dispersion curves for the 4-cell PWT structure.

III. COLD TESTS ON PWT1

Because of a fabrication error, the tank of the first prototype PWT linac structure was about 13 mm longer than the designed length resulting in one of the end half-cells being longer than the other end half-cell by the same amount [11,12]. From the tolerance map we could predict that this should cause a reduction of about 50 MHz in the resonant frequency of the structure. To confirm this, the structure was simulated using GDFIDL for the dimensions of the actual fabricated structure and a resonant frequency of 2916 MHz was obtained for the structure. To verify this, cold tests were done on the structure using a HP Vector Network Analyzer (HP8753E) at an input power level of 10 mW. The transmission method was used for frequency measurements with the rf and vacuum ports used for coupling microwave power into and out of the structure, respectively. Magnetic field coupling was employed using a loop, which was located at a point giving a very weak coupling.

The frequency spectrum of the structure was obtained for a wide range of frequency for the prototype PWT1 structure. The operation "π" mode is found to be at 2903 MHz, which is within $<0.5\%$ of the resonant frequency of 2916 MHz predicted by GDFIDL.

A bead-pulling test using a dielectric bead (Teflon) was performed to confirm that this resonant frequency corresponds to the π mode of operation by employing phase as well as frequency perturbation techniques. The bead-pull setup consists of a 3D motion stand over which the PWT structure is fitted with an arrangement of pulleys to pull

TABLE I.   Comparison of various rf parameters of the prototype PWT1 linac obtained from SUPERFISH and GDFIDL simulations.

rf parameters	SUPERFISH results	GDFIDL results
Resonant frequency, f_0	2856 MHz	2969 MHz
Quality factor, Q_0	27 770	22 267
Effective shunt impedance, $R_s T^2$	39 MΩ/m	46 MΩ/m
Characteristic impedance, r/Q_0	1405 Ω/m	2083 Ω/m

the nylon thread through the structure. A small cylindrical bead (5 mm length, 5 mm radius) of Teflon was fixed on the nylon thread and a controlled stepper motor was used to move the bead in steps inside the structure. The dielectric bead inside the structure perturbed the resonant frequency corresponding to the electric field value at that point.

The quality factor of the structure for the operation mode was found to be about 14 000 and the characteristic impedance was around 468 Ω [13].

IV. THE SECOND PROTOTYPE (PWT2)

In order to have a better idea of the agreement between cold-test results and those predicted by GDFIDL simulations, we made sets of dummy disks of different diameters from electrolytic tough pitch Cu, which were mounted inside the tank structure of the prototype PWT1, which is 13 mm longer than the designed value due to machining errors in fabrication. The resonant frequencies for disks of different diameters were calculated using GDFIDL and compared with those obtained from cold tests. It can be seen from Table II that there is reasonably good agreement between the two. These measured results are matching within 0.5% of the predicted resonant frequency using GDFIDL.

The diameter of the disks for the prototype PWT2 structure was increased to 88 from 85.2 mm for the PWT1 structure. The simulated value of the resonant frequency for the second prototype was 2884 MHz, while that measured in cold tests was 2885 MHz, showing a very good agreement. We repeated this test many times by using a spectrum analyzer. A series of cold tests was performed using different tank sizes and disk diameters in addition to doing many simulations to design a structure resonating at 2856 MHz.

V. THE THIRD PROTOTYPE (PWT3)

With a slight modification in the design of the PWT2 structure by increasing the disk outer diameter to 90.0 mm and PCD [10] of the holes for support tubes to 74.5 mm, the PWT3 structure was simulated to resonate at a frequency of 2858 MHz. A frequency higher than the desired resonant frequency of 2856 MHz was targeted as fine-tuning to a few MHz could be done to reduce the frequency

TABLE II. Comparison of predicted and measured resonant frequencies as a function of the disk diameter.

Disk diameter (mm)	Resonant frequency (MHz)	
	GDFIDL prediction	Cold-test measurements
85.2	2916	2903
86.0	2911	2908
87.0	2905	2907
88.0	2897	2896
89.0	2892	2888
90.0	2883	2879
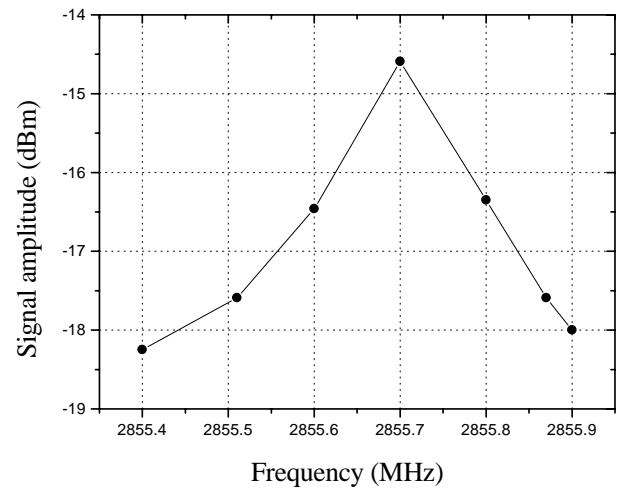
FIG. 7.   Frequency spectrum of the PWT3 linac structure.

by increasing the length of an end half-cell of the structure, while the reduction in the structure length is not possible to increase the resonant frequency of the fabricated structure. The PWT3 structure was cold tested using a different setup than what was used for PWT2 and PWT1. A Rohde & Schwarz make (model SMT03) signal generator was used to launch the rf at a 10 dBm power level into the structure using a coax-waveguide adaptor. The field inside the structure was sampled by using a magnetically coupled loop antenna, from which the signal was fed to a Boonton make power meter (model 4531). Since the frequency from the signal generator could be varied very finely, it allowed for accurate measurement of the amplitude of the field's setup inside the structure for different frequencies. Figure 7 shows the variation of field amplitude inside the structure with the frequency indicating a resonant frequency of 2855.7 MHz for the structure of total length 212.0 mm. In the PWT3 structure, the end cell was increased by a few mm to tune the structure near to 2856 MHz, hence the field amplitude decreased in this end cell as well in the neighboring cells. Figure 8 shows the results obtained from the bead perturbation measurements,
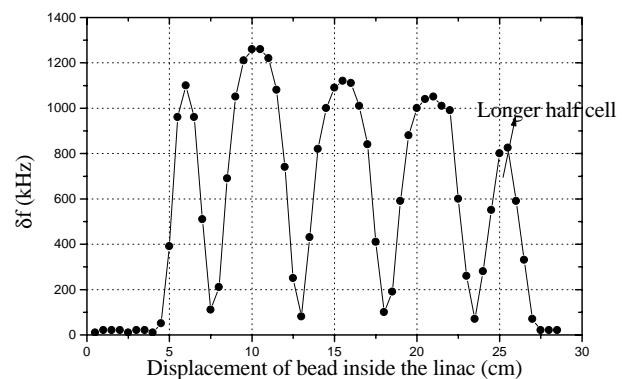
FIG. 8.   Frequency deviation from the resonant frequency in the bead-pull test of the PWT3 linac structure.

showing the operating mode at 2855.7 MHz to be the π mode.

VI. BEAM DYNAMICS SIMULATIONS

We used PARMELA for the particle beam dynamics study in a PWT linac structure. PARMELA is a versatile multi-particle code that transforms the beam through a specified linac/transport line. It does a 2D space charge calculation and an optional 3D point-to-point space charge calculation [9]. These simulations were performed with 10 000 super particles having a normal distribution, and assuming a relativistic electron beam (5 MeV) with no initial divergence and emittance at the input end of the structure. The beam input parameters are listed in Table III. PARMELA simulations considered a beam pulse of 1 nC charge in a 10 ps pulse giving 100 A of peak current.

Simulations were performed to follow the beam energy gain and emittance growth in the structure since for high-brightness electron beam acceleration, the study of emittance becomes very important. Figure 9 shows the energy gain of the electron beam in the PWT structure, which is a linear function of the field gradient. PARMELA simulations predict the 90% normalized rms emittance at the exit of the PWT1 linac to be 1.565 mm mrad for initial beam parameters listed in Table III. When the space charge calculation is turned off, 90% normalized rms emittance is 0.572 mm mrad at the end of the first half-cell of the PWT1 linac structure, and 0.376 mm mrad at the exit of the end half-cell of the structure. This shows that the accelerating field reduces the emittance in the acceleration process quite significantly. In other simulations, we tried to get the effect of the space charge on the emittance of the beam by keeping the field gradient as zero. For this case, the emittance at the end of the first half-cell is 0.639 mm mrad, and at the exit of the linac the normalized 90% rms emittance is 2.731 mm mrad. It can be seen that the space charge has more impact on emittance growth. However, since the beam is already relativistic as it enters into the PWT structure, the actual effect of space charge forces is not very strong.

When space charge effect is turned off, the emittance of the beam increases with field gradient, while in the presence of space charge but with zero field gradient, emittance

TABLE III.   Input beam parameters for PARMELA simulations.

Parameters	Values at input end of PWT structure
Bunch charge	1 nC
Bunch length	10 ps
Bunch distribution	Gaussian
Peak current	100 Amps
Initial energy	5 MeV
Average field gradient	32 MV/m
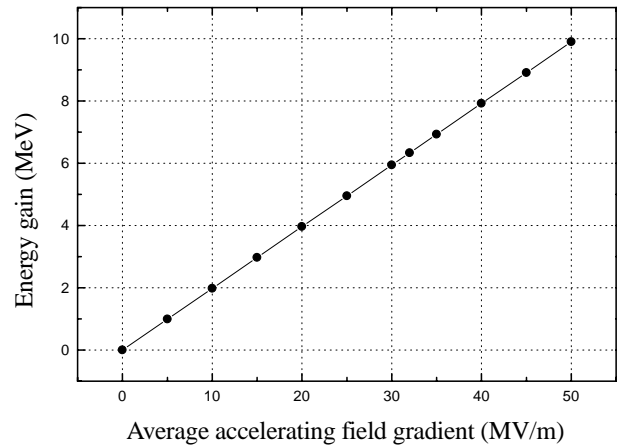
FIG. 9.   Energy gain vs accelerating field in the 4-cell, PWT linac structure.

grows in the structure purely due to space charge effect. These effects can be seen in Figs. 10 and 11. The increase in emittance is very small in the zero-space charge regime (cf. lower curve in Fig. 10). When both the space charge effect and the rf field gradient are not zero, it is seen that the interaction between the two causes the emittance increase due to space charge effect to be suppressed by the field gradient by an amount larger than the increase in emittance purely due to the rf field gradient (cf. upper curve in Fig. 10). For a 1 nC charge in a 10 ps pulse, the emittance reduces with the increase in the accelerating field gradient (cf. Fig. 11). This is due to the reduction in the space charge effect at high field gradients and at high bunch speed.

The emittance increases in the acceleration process inside the PWT structure and is shown in Fig. 12 with different pulse charges and accelerating field gradients. In the zero charge (space charge effect off) case, the accelerating field gradient compresses the bunch in the radial direction, while the presence of the space charge causes an increase in divergence and consequently the size of the
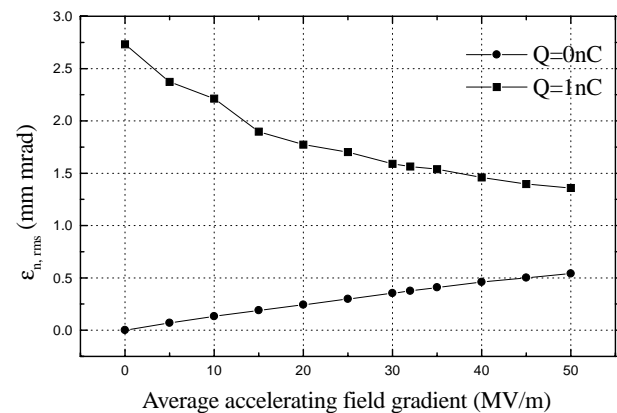
FIG. 10.   Emittance growth in the PWT linac structure with accelerating field gradient for different pulse charges.
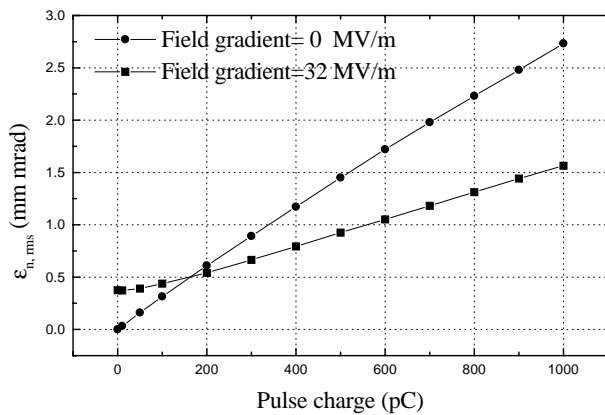
FIG. 11.   Emittance growth in the PWT structure with beam pulse charge.
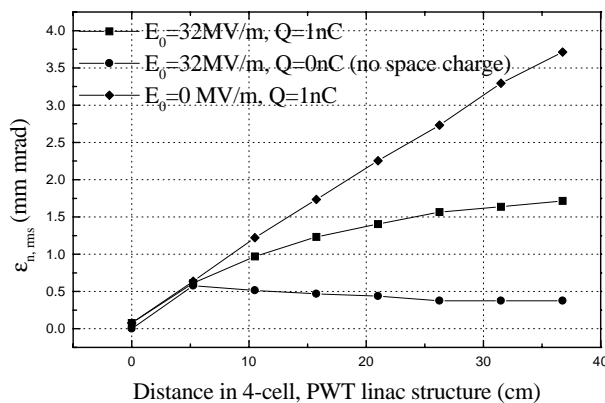
FIG. 12.   Emittance variation in the 4-cell, PWT linac structure with different accelerating field gradients and pulse charges.

beam. It should be noted here that the initial beam parameter does not consider any divergence in the electron beam and considers zero emittance of the electron beam pulses. As mentioned earlier, these structures are planned to be used for the acceleration of a high-brightness electron beam generated by a photocathode rf gun. Hence, initial beam parameters are taken to be the same as a beam coming out from a photocathode rf gun with 5 MeV beam energy [14]. It is also predicted by PARMELA simulations that the bunch length also gets affected due to space charge effects. Hence, for getting a very high peak beam current, the electron beam pulses have to be compressed.

VII. CONCLUSIONS

The prototype PWT structures we have described in this paper solved many issues related to the fabrication of the actual accelerating structure proposed to be built at CAT. We have done detailed tolerance analysis of the PWT structure. From these studies, it has been found that it is im-

portant to locate the supporting/cooling tubes on the disks precisely in a region to cause a minimum perturbation in resonant frequency and in power dissipation.

The design and fabrication of the prototypes of the PWT structure have been done to establish and improve in-house technology for the development of high-brightness electron beam accelerators for FEL applications and to meet the challenges posed by the future experiments requiring a high quality beam. We have now successfully built a PWT structure that resonates at 2856 MHz with a quality factor Q of around 10 000. Our next step is to hot test the structure and look for dark current acceleration. After this, we shall inject an electron beam from a 70 keV thermionic electron gun and accelerate the beam to around 4 MeV.

[1] J. S. Fraser, R. L. Sheffield, E. R. Gray, and G. W. Rodenz, IEEE Nucl. Sci. **32**, 1791–1793 (1985); L. Serafini, R. Zhang, and C. Pellegrini, Nucl. Instrum. Methods Phys. Res., Sect. A **387**, 305–314 (1997); D. T. Palmer *et al.*, in *Proceedings of the Particle Accelerator Conference, Dallas, Texas, 1995* (IEEE, Piscataway, NJ, 1996).

[2] R. Zhang, C. Pellegrini, and R. Cooper, Nucl. Instrum. Methods Phys. Res., Sect. A **394**, 295–304 (1997).

[3] Donald A. Swenson, in *Proceedings of the European Particle Accelerator Conference, Rome, 1988* (World Scientific, Singapore, 1988), pp. 1418–1420.

[4] R. Zhang, P. Davis, G. Hairapetian, M. Hogan, C. Joshi, M. Lampel, S. Park, C. Pellegrini, J. Rosenzweig, and G. Travish, in *Proceedings of the Particle Accelerator Conference, Dallas, Texas, 1995* (Ref. [1]), p. 1102.

[5] V. G. Andreev *et al.*, in *Proceedings of the International Conference on High Energy Accelerators, Frascati, Italy, 1965* (CNEN, Roma, 1966); V. G. Andreev, Sov. Phys. Tech. Phys. **13**, 1070 (1969).

[6] R. Zhang, Ph.D. thesis, University of California, Los Angeles, 1997.

[7] K. Halbach and R. F. Holsinger, Part. Accel. **7**, 213–222 (1976).

[8] W. Bruns, in *Proceedings of the Particle Accelerator Conference, Vancouver, Canada, 1997* (IEEE, Piscataway, NJ, 1998), p. 2651.

[9] Computer code PARMELA, in Lloyd M. Young, Los Alamos National Laboratory Report No. LA-UR-96-1835.

[10] Pitch circle diameter (PCD) is the diameter of the circle passing through the centers of the four holes for supporting tubes on each disk.

[11] Arvind Kumar, K. K. Pant, and S. Krishnagopal, Centre for Advanced Technology Report No. CAT/2000-14, 2000.

[12] K. K. Pant, V. Prasad, and S. Krishnagopal, Centre for Advanced Technology Report No. CAT/2000-08, 2000.

[13] Arvind Kumar, K. K. Pant, and S. Krishnagopal, Centre for Advanced Technology Report No. CAT/2000-21, 2000.

[14] D. T. Palmer, Ph.D. thesis, Stanford University, Stanford, CA, 1998.